REPORT

# Biallelic *IARS* Mutations Cause Growth Retardation with Prenatal Onset, Intellectual Disability, Muscular Hypotonia, and Infantile Hepatopathy

Robert Kopajtich,[1,2,19] Kei Murayama,[3,4,19] Andreas R. Janecke,[5,6,19] Tobias B. Haack,[1,2,19] Maximilian Breuer,[7,19] A.S. Knisely,[8,9] Inga Harting,[10] Toya Ohashi,[11] Yasushi Okazaki,[12,13] Daisaku Watanabe,[14] Yoshimi Tokuzawa,[13] Urania Kotzaeridou,[7] Stefan Kölker,[7] Sven Sauer,[7] Matthias Carl,[15] Simon Straub,[5] Andreas Entenmann,[5] Elke Gizewski,[16] René G. Feichtinger,[17] Johannes A. Mayr,[17] Karoline Lackner,[9] Tim M. Strom,[1,2] Thomas Meitinger,[1,2] Thomas Müller,[5] Akira Ohtake,[18] Georg F. Hoffmann,[7] Holger Prokisch,[1,2] and Christian Staufner[7,*]

tRNA synthetase deficiencies are a growing group of genetic diseases associated with tissue-specific, mostly neurological, phenotypes. In cattle, cytosolic isoleucyl-tRNA synthetase (*IARS*) missense mutations cause hereditary weak calf syndrome. Exome sequencing in three unrelated individuals with severe prenatal-onset growth retardation, intellectual disability, and muscular hypotonia revealed biallelic mutations in *IARS*. Studies in yeast confirmed the pathogenicity of identified mutations. Two of the individuals had infantile hepatopathy with fibrosis and steatosis, leading in one to liver failure in the course of infections. Zinc deficiency was present in all affected individuals and supplementation with zinc showed a beneficial effect on growth in one.

Aminoacyl-tRNA synthetases (ARSs) catalyze the aminoacylation of tRNAs by their cognate amino acid, linking amino acids with the correct nucleotide triplets and ensuring the correct transformation of the genetic code to the protein level. Editing activities of ARSs further increase translation fidelity by preventing misacylation of tRNAs with non-cognate amino acids.[1] In mammals, ARSs can be distinguished by their cytoplasmatic or mitochondrial localization, with only two ARS in both compartments (GARS and KARS). In 2003, autosomal-dominant Charcot Marie Tooth disease (CMT) type 2D (MIM: 601472) and neuropathy, distal hereditary motor, type VA (MIM: 600794), caused by mutations in *GARS* (MIM: 600287, encoding glycyl-tRNA synthetase) were reported as the first ARS-associated human disease phenotypes.[2] Since then, several clinical conditions associated with mutations in mitochondrial ARSs[3,4] and cytosolic ARSs[5] have been identified. Clinically, most cytosolic tRNA synthetase deficiencies are associated with CMT and related neuropathies,[1] whereas mutations in *LARS* (MIM: 151350) cause infantile acute liver failure syndrome type 1 (MIM: 615438)[6] and autosomal-recessive mutations in *MARS* (MIM: 156560) cause interstitial lung and liver disease (MIM: 615486).[7]

Mutations in cytosolic *IARS* (MIM: 600709) have not yet been linked to human disease. However, a homozygous missense mutation (c.235G>C) in exon 3 has recently been identified as the molecular cause of weak calf syndrome in Japanese black cattle.[8] The affected calves exhibit prenatal-onset growth retardation, severe muscle weakness with astasia, and fatty degeneration of liver cells.[8,9]

Here we report the identification of biallelic mutations in *IARS* in three unrelated individuals with a complex multisystemic phenotype of prenatal-onset growth retardation (3/3), intellectual disability (3/3), muscular hypotonia (2/3), and hepatopathy with fibrosis and steatosis (2/3) as well as diabetes mellitus and sensorineural hearing loss (1/3). The three individuals studied originate from Germany (#65269, DEU), Japan (#85880, JPN), and Austria (#83921, AUT). Clinical findings are summarized in Table 1 (for anthropometrical data see Table S1).

Individual #65269 (DEU), a boy, was born at 38 weeks' gestational age to non-consanguineous German parents. Birth weight and head circumference were low (weight

[1]Institute of Human Genetics, Helmholtz Zentrum München, 85764 Neuherberg, Germany; [2]Institute of Human Genetics, Technische Universität München, 81675 Munich, Germany; [3]Department of Metabolism, Chiba Children's Hospital, Chiba 266-0007, Japan; [4]Chiba Cancer Center Research Institute, Chiba 260-8717, Japan; [5]Department of Pediatrics I, Medical University of Innsbruck, 6020 Innsbruck, Austria; [6]Division of Human Genetics, Medical University of Innsbruck, 6020 Innsbruck, Austria; [7]Department of General Pediatrics, Division of Neuropediatrics and Metabolic Medicine, University Hospital Heidelberg, 69120 Heidelberg, Germany; [8]Institute of Liver Studies, King's College Hospital, London SE5 9RS, UK; [9]Institute of Pathology, Medical University of Graz, 8036 Graz, Austria; [10]Department of Neuroradiology, University Hospital Heidelberg, 69120 Heidelberg, Germany; [11]Department of Pediatrics, The Jikei University School of Medicine, Tokyo 105-8461, Japan; [12]Division of Translational Research, Research Center for Genomic Medicine, Saitama Medical University, Hidaka, Saitama 350-1241, Japan; [13]Division of Functional Genomics & Systems Medicine, Research Center for Genomic Medicine, Saitama Medical University, Hidaka, Saitama 350-1241, Japan; [14]Department of Large Animal Clinics, School of Veterinary Medicine, Kitasato University, Towada, Aomori 034-8628, Japan; [15]Department of Cell and Molecular Biology, Medical Faculty Mannheim, Heidelberg University, 68167 Mannheim, Germany; [16]Department of Neuroradiology, Medical University of Innsbruck, 6020 Innsbruck, Austria; [17]Department of Paediatrics, Paracelsus Medical University, SALK Salzburg, 5020 Salzburg, Austria; [18]Department of Pediatrics, Faculty of Medicine, Saitama Medical University, Moroyama, Saitama 350-0495, Japan
[19]These authors contributed equally to this work
*Correspondence: christian.staufner@med.uni-heidelberg.de
http://dx.doi.org/10.1016/j.ajhg.2016.05.027.

**Table 1. Genetic and Clinical Findings in Individuals with *IARS* Mutations**

| | | | *IARS* Mutations | | Clinical Features | | | |
|---|---|---|---|---|---|---|---|---|
| ID | Sex | Age at Last Visit | cDNA (NM_002161.5); protein (EAW62813.1) | AO | Growth Retardation (SDS)[a] | Neurological and Cognitive Outcome | Liver Function (Histologic Findings) | Other Features |
| #65269 (DEU) | M | 18.7 years | c.[1252C>T];[3521T>A]; p.[Arg418*];[Ile1174Asn] | prenatal (IUGR) | yes (−5.9) | moderate to severe intellectual disability, no expressive speech, spastic movement disorder (GMFCS IV), muscular hypotonia, brain MRI abnormal | intermittently mildly affected hepatic synthesis (no liver biopsy) | strabismus, feeding through PEG, esophagitis, zinc deficiency (8.5 μmol/L; N 13–18)[b] |
| #85880 (JPN) | F | 19 years | c.[760C>T];[1310C>T]; p.[Arg254*];[Pro437Leu] | prenatal (IUGR) | yes (−6.2) | moderate intellectual disability (IQ 50), motor function normal | elevated ALAT and ASAT, neonatal onset (steatosis, fibrosis) | sensoneurinal hearing loss (AO 5 years), diabetes mellitus (AO 16 years), epilepsy, zinc deficiency (7.5 μmol/L; N 11–18)[b] |
| #83921 (AUT) | M | 3 years | c.[1109T>G];[2974A>G]; p.[Val370Gly];[Asn992Asp] | prenatal (IUGR) | yes (−6.2) | moderate intellectual and motor disability, muscular hypotonia | recurrent liver crises triggered by infections, infantile liver failure, neonatal onset (steatosis, fibrosis, cholestasis) | peculiar facial distribution of subcutaneous fat (chubby cheeks), feeding through PEG, zinc deficiency (6.1 μmol/L; N 11–15)[b] |

Abbreviations are as follows: M, male; F, female; AO, age of onset; IUGR, intrauterine growth retardation; GMFCS, gross motor function classification system; PEG, percutaneous endoscopic gastrostomy; N, normal range.
[a]Minimum SDS value of body height.
[b]Minimum value measured in blood.

2,020 g, −3.0 SDS; head circumference 29.0 cm, −4.2 SDS; see Table S1). He has two healthy sisters. Pregnancy was normal except for intrauterine growth retardation. Substantial psychomotor retardation, muscular hypotonia, and poor feeding were noted shortly after birth and despite alimentation by percutaneous gastroenterostomy with a high-calorie diet, failure to thrive was very severe (at 6 years of age, body weight 10.8 kg, −8.0 SDS). During the first 2 to 3 years, multiple clinically severe infections occurred. At the age of 7 years, zinc deficiency was detected in serum (8.5 μmol/L; normal range 13–18) and zinc supplementation was begun (1 mg/kg body weight/day). Normalization was associated with pronounced improvement in clinical status. He had fewer infections; weight, height, and head circumference increased substantially (see Figure S1); and both hypoalbuminemia and low levels of growth hormone-dependent factors IGF1 and IGFBP3 normalized. Psychomotor development also seemed to improve: the child became more alert and mobile and progressively took increasing part in various daily activities. Examination at the age of 17 years revealed lack of expressive speech with moderate to severe intellectual disability, muscular hypotonia, and bilateral spasticity (Gross Motor Function Classification System Level IV). However, he understood commands, interacted with others, and performed some activities. Weight and height had become nearly normal (−2.8 SDS resp. −1.6 SDS), whereas microcephaly was still pronounced (−5.1 SDS). Brain MRI showed white matter changes consistent with hypomyelination (Figure S2).

Individual #85880 (JPN), a girl, was born at 38 weeks' gestational age, the third child of non-consanguineous Japanese parents. A brother is healthy. A sister has mild intellectual disability. Birth weight and head circumference were low (1,564 g, −4.1 SDS; 29 cm, −3.5 SDS). Pregnancy was normal except for intrauterine growth retardation. At the age of 4 days, mildly elevated transaminase activities (ALAT, ASAT) and a normal to slightly reduced prothrombin time were observed. These spontaneously improved until 6 years of age. Liver biopsy at 2 years of age showed steatosis and portal-tract fibrosis with evidence of accelerated hepatocyte turn-over in absence of other usual histopathologic features of hepatitis or steatohepatitis (Figure S3). The girl had global developmental delay (sitting at 15 months of age, walking at 2 years of age). At the age of 5 years, severe sensorineural hearing loss was diagnosed. Body growth was retarded (with documented growth hormone deficiency). Growth hormone therapy between the ages of 3 4/12 years and 14 years resulted in normalization of growth. She had an unexplained episode of unconsciousness and two episodes of afebrile generalized tonic-clonic seizures for a few minutes at 14 and 16 years. Electroencephalograms were unremarkable and no antiepileptic drug therapy was initiated. Insulin-dependent diabetes mellitus was diagnosed at 16 years of age and insulin therapy was started. Brain MRI was normal at the age of 16 years. At this writing, she is 21 years old and has mild to moderate intellectual disability (verbal IQ 47, performance IQ 50). She has no microcephaly. Liver function is normal. Recurrent infection is not a problem.

Individual #83921 (AUT), a boy, was born at 38+4 weeks' gestational age to non-consanguineous Austrian parents. Birth weight and head circumference were both low (2,700 g, −1.6 SDS; 30 cm, −3.8 SDS). Pregnancy was normal except for intrauterine growth retardation. At the age of 3 weeks, jaundice became apparent and conjugated hyperbilirubinemia, mildly elevated ALAT and ASAT, but normal γGT and mild hypoalbuminemia were identified. Liver biopsy found non-specific changes labeled as "neonatal hepatitis." Jaundice spontaneously disappeared at the age of 5 months. In the second year of life, three episodes of marked conjugated hyperbilirubinemia, moderate coagulopathy, markedly elevated ALAT and ASAT, but normal γGT were encountered in the context of a gastrointestinal and two respiratory infections. Liver biopsy at 14 months of age showed cholestasis, steatosis with steatohepatitis, portal-tract fibrosis with bridging in a biliary rather than post-necrotic pattern, and evidence of accelerated hepatocyte turn-over (Figure S4). At the age of 2 years, an upper respiratory tract infection was accompanied by acute liver failure (conjugated bilirubin 10.2 mg/dL, normal < 0.3; ALAT 360 U/L, ASAT 1,700 U/L, normal < 50; γGT 16 U/L, normal < 21; INR 2.7, normal < 1.2) complicated by candida sepsis and requiring intensive-care support. After recovery, he had an episode of prolonged conjugated hyperbilirubinemia with low serum γGT associated with an infection. After recovery from infections, serum albumin levels ranged from low to normal and coagulation parameters normalized. During episodes of liver dysfunction, the boy appeared to benefit from a high-calorie diet. Alimentation was generally difficult: despite high-calorie tube feeding, weight and height remained below the 3$^{rd}$ percentile and at 2 years of age (height −6.2 SDS, weight −3.5 SDS, head circumference −4.4 SDS) a percutaneous gastrostomy was placed. On high-calorie stomal feeding the boy throve better, with improved motor skills, but vomiting was a problem. Zinc deficiency was diagnosed at 2 6/12 years of age and zinc supplementation was started (1–2 mg/kg body weight/day). Zinc levels fluctuated markedly (minimum 6.1 μmol/L) but tended to be slightly below the normal range despite supplementation. Supplementation with isoleucine (200 mg/kg/day) also was started and alimentation increased. The boy has thereafter appeared less susceptible to infection, with better development. Psychomotor development was delayed; at the age of 2 years, the child performed at the level of a 12-month-old infant. No abnormality was identified on brain MRI at the age of 2 3/12 years. At this writing, the boy is 3.5 years old. He is short (−5.0 SDS) and microcephalic (−3.3 SDS), but BMI is normal (+1.0 SDS).

In all three individuals, a mitochondrial disease was suspected clinically and respiratory chain complexes were measured in muscle (subjects DEU and AUT), liver (subject AUT), and/or fibroblasts (subjects DEU and JPN) (see Table S2). Activities of complex I appeared to be decreased in the three subjects in at least one tissue, whereas activity of complex IV was decreased in one. Thorough clinical and metabolic investigations were without specific findings in all cases. Transient elevations of plasma lactate concentrations were found. However, plasma lactate was also repeatedly normal in all individuals and brain magnetic resonance spectroscopy (MRS), performed in subjects DEU and AUT at the age of 17 and 2 years, showed no lactate peaks.

Informed consent to participate in the study was obtained from all affected individuals or their parents in case of minor study participants. The study was approved by the ethics committees of the University Hospital Heidelberg, the Technische Universität München, the Jikei University School of Medicine, Chiba Children's Hospital and Saitama Medical University, and the Medical University of Innsbruck. Whole-exome sequencing performed on genomic DNA from individual #65269 (DEU) did not identify likely clinically relevant variants in genes previously associated with the observed clinical phenotype or a mitochondrial disorder.[10,11] A search for homozygous or potentially compound heterozygous rare variants (MAF < 0.1% in 7,000 in-house exomes, 1000 Genomes Study) prioritized the five genes *PROB1*, *UBR2* (MIM: 609134), *IARS*, *PLXNB3* (MIM: 300214), and *DUSP21* (MIM: 300678). Given the overlap of clinical features of the investigated individual with the phenotypic spectrum of other ARS defects, we considered *IARS* a strong candidate. Results of two independent exome sequencing studies that revealed biallelic *IARS* variants in two unrelated individuals from Austria and Japan with phenotypic features like those in the German boy supplied further evidence for a causal association of biallelic *IARS* variants with the disease presentation. All six identified *IARS* variants were confirmed by Sanger sequencing. Carrier testing confirmed a compound heterozygous state of the *IARS* variants (Figure 1). Except for the variant c.1252C>T, which was detected three times in a heterozygous state, none of the *IARS* variants (c.760C>T, c.1109T>G, c.1310C>T, c.2974A>G, and c.3521T>A) was listed in >120,000 alleles of the Exome Aggregation Consortium (ExAC) Server (12/2015). All the missense mutations change evolutionarily conserved amino acid residues (Figure 1) and are accordingly predicted to be damaging (PolyPhen-2 and SIFT). Immunoblotting analysis of fibroblast cell extracts from all three affected individuals showed reduced levels of IARS protein only for subject #65269 (DEU; see Figure S5). Immunostaining of formalin-fixed, paraffin-embedded archival liver-biopsy material (JPN, AUT) found no marking for IARS in one (JPN) and normal marking in the other (AUT; Figure S6). Four of the six mutations lie in the first half of the gene, in close proximity to the IleRS core domain (Figure 1).

To evaluate the functional relevance of identified *IARS* variants, we made use of a Tet-Off yeast model.[12] In the TET-ILS1 strain, expression of *ILS1*, the *Saccharomyces cerevisiae* ortholog of human *IARS*, can be negatively regulated by addition of doxycycline to the growth medium. The strain shows normal growth under standard

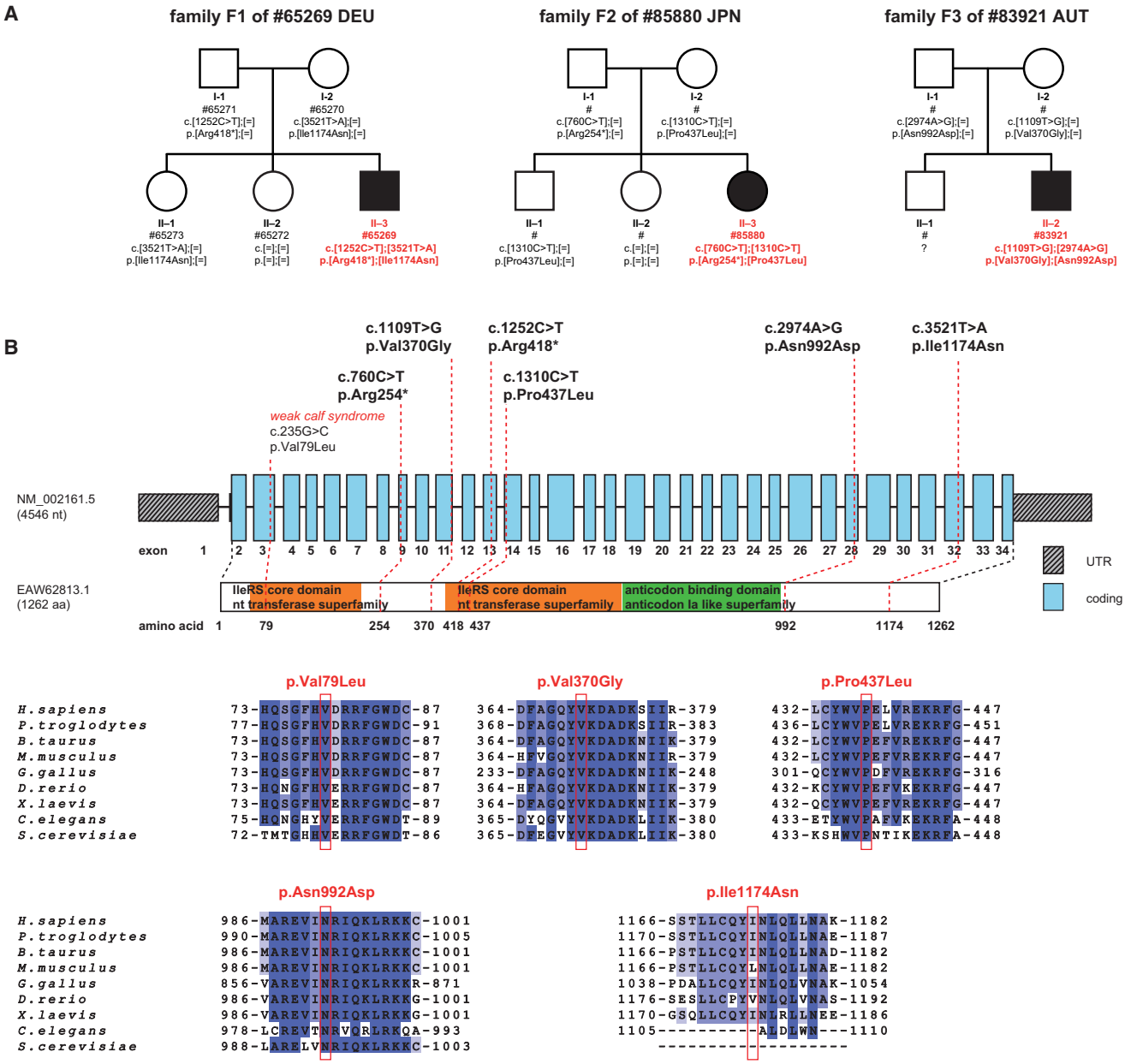


**Figure 1.** ***IARS*** **Variants and Gene Structure**
(A) Pedigrees of the three families with recessive inherited mutations in *IARS*.
(B) Structure of *IARS* with known conserved protein domains in the gene product and localization and conservation of amino acid residues affected by mutations identified in the three families as well as by the orthologous-gene mutation associated with the weak calf syndrome. Intronic regions are not drawn to scale. Coloring in the sequence alignment represents the identity of amino acid residues.

conditions (Figure 2). Reduced expression of *ILS1* resulted in considerable growth impairment; however, this phenotype was fully rescued by expression of the human wild-type *IARS* cDNA (Figure 2, first two lines) providing an in vivo assay to evaluate mutant alleles. *IARS* cDNAs carrying the different variants were cloned into the low-copy vector pYX122 (Novagen) and growth was compared to that of cells transformed with a wild-type copy of *IARS* or with the empty vector.

Without addition of doxycycline, the transformed yeast strains grew like the positive control. Upon downregulation of the yeast IARS ortholog, no growth rescue was observed in yeast transformed with empty vector (negative control), plasmids encoding the two *IARS* loss-of-function variants c.1252C>T (p.Arg418*) (#65269, DEU) and c.760C>T (p.Arg254*) (#85880, JPN), or a plasmid encoding the missense variant c.2974A>G (p.Asn992Asp) (#83921, AUT). An intermediate growth phenotype was obtained by expression of the four missense variants c.235G>C (p.Val79Leu) (not encountered in any proband; the ortholog of that in *IARS* in cattle, which underlies weak calf syndrome), c.3521T>A (p.Ile1174Asn) (#65269, DEU), c.1310C>T (p.Pro437Leu) (#85880, JPN), and c.1109T>G (p.Val370Gly) (#83921, AUT); the last displayed the

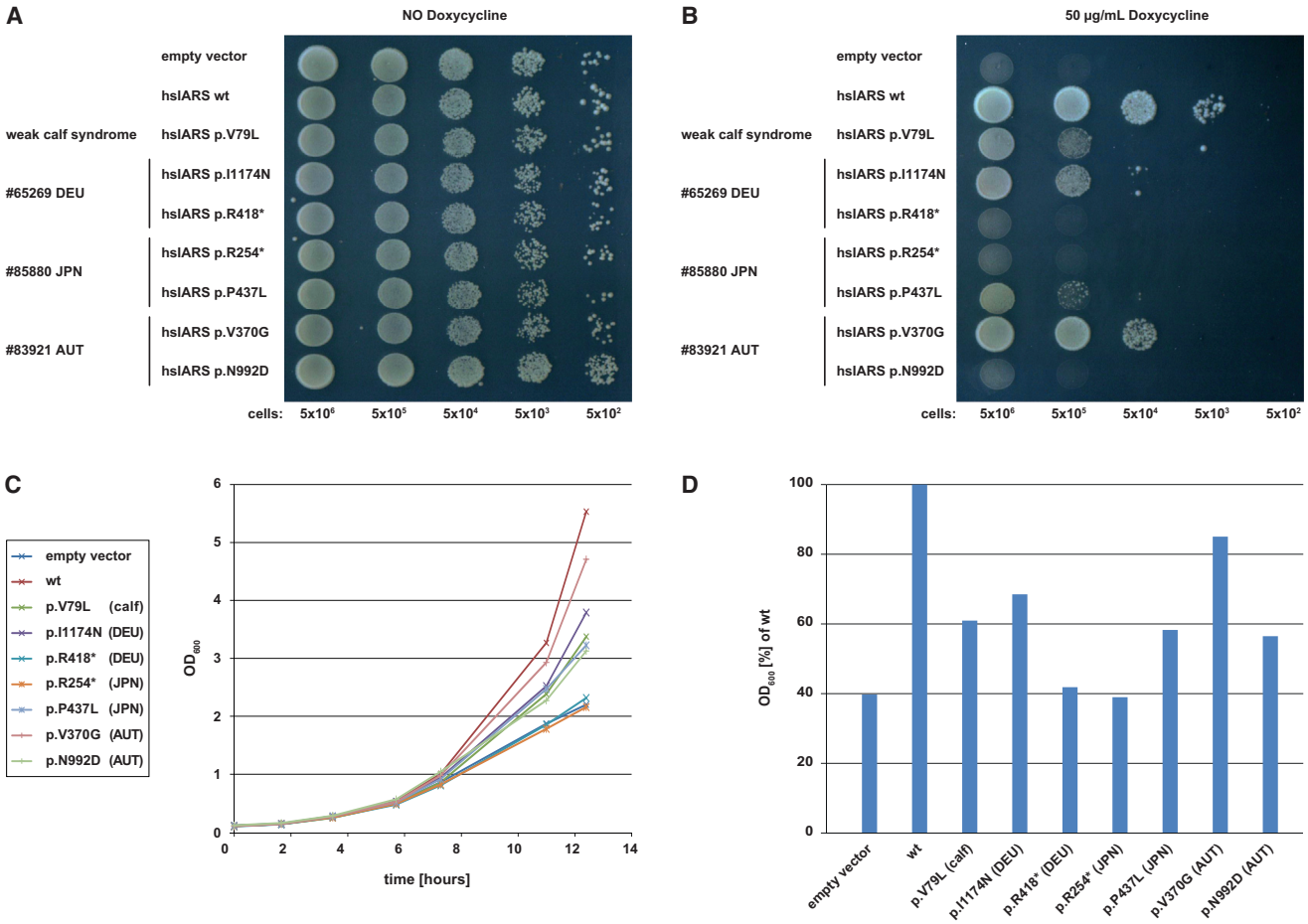


**Figure 2. Yeast Studies**

Spot assay and growth curves of TET-ILS1 strain, transformed with the low copy vector pYX122 (Novagen) containing different mutated versions of human *IARS* cDNA encoding the protein products "hsIARS WT," pYX122:h*IARS*$^{wt}$; "hsIARS V79L," pYX122:*hiars*$^{p.Val79Leu}$; "hsIARS I1174N," pYX122:*hiars*$^{p.Ile1174Asn}$; "hsIARS R418*," pYX122:*hiars*$^{p.Arg418*}$; "hsIARS R254*," pYX122:*hiars*$^{p.Arg254*}$; "hsIARS P437L," pYX122:*hiars*$^{p.Pro437Leu}$; "hsIARS V370G," pYX122:*hiars*$^{p.Val370Gly}$; and "hsIARS N992D," pYX122:*hiars*$^{p.Asn992Asp}$. Empty vector "pYX," pYX122, was used as a negative control. Decreasing numbers of yeast cells ($5 \times 10^6$, $5 \times 10^5$, $5 \times 10^4$, $5 \times 10^3$, $5 \times 10^2$) were spotted onto plates containing drop-out medium (SC-His). Growth curves were obtained in liquid cultures with SC-His medium by monitoring $OD_{600}$. Downregulation of yeast *ILS1* was induced by addition of 50 mg/mL doxycycline.

(A) Expression of the different *IARS* WT and mutant constructs in the TET-ILS1 strain did not show any negative effect on growth.

(B) Downregulation of *ILS1* led to failure in growth that could be rescued by expression of human wild-type *IARS*. Each affected individual carries one loss-of-function allele in combination with one allele that displays residual activity as measured by growth. Transformation with a construct encoding the variant associated with the perinatal weak calf syndrome resulted in partial rescue of the growth defect.

(C) Growth in liquid culture. Cells grown overnight were inoculated into fresh medium containing doxycycline. $OD_{600} = 0.1$; growth monitored at 30°C.

(D) Optical density after 12.5 hr of growth, expressed as percentage of WT. All variants significantly impaired the growth rate (Wilcoxon test, $p < 0.05$).

Representative data are shown.

mildest, but significant, growth impairment (Figure 2). Hence, each affected human individual is compound heterozygous for an *IARS* loss-of-function allele and an allele with significantly reduced but some remaining functionality, similar to the allele causing weak calf syndrome. Treatment with zinc appeared beneficial in subject #65269 (DEU), possibly due to zinc deficiency or to zinc dependence of IARS activity, as shown for the *E. coli* ortholog.[13] Supplementation using a wide range of zinc concentrations did not improve yeast growth, permitting argument that zinc has no direct effect on IARS activity.

To gain further insight into the expression pattern of *IARS* and its role for embryonic development, we undertook in situ hybridization and morpholino (MO) knockdown of *iars* in zebrafish. Iars is conserved in zebrafish and shares 74% homology to the human protein. The expression of *iars* is ubiquitous in zebrafish during early embryonic development. It localizes to the somites and developing brain regions after gastrulation, especially in the tectum region of the brain, pineal gland, and hindbrain (Figure 3). To assess Iars function, two splice-blocking MOs specific to *iars* were injected into zebrafish embryos. MO specificity was

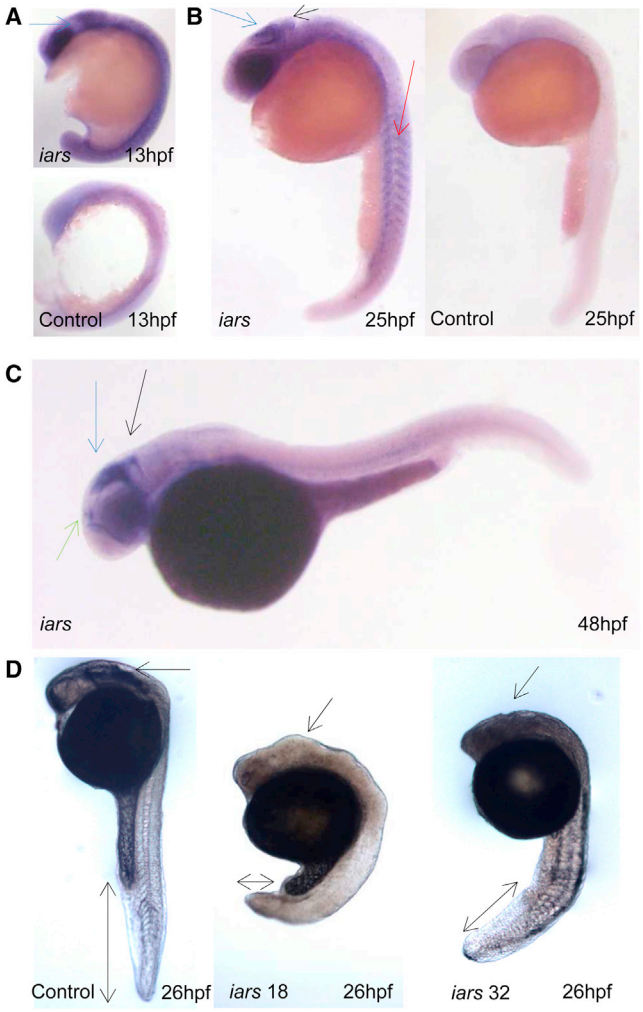


**Figure 3. In Situ Hybridization and Morpholino Knockdown of *iars* in Zebrafish**

Zebrafish were maintained[35] and embryos were staged as described.[36] Embryos older than 24 hr after fertilization (hpf) were treated with 0.0003% phenylthiourea (Sigma) to inhibit pigment synthesis and fixed in 4% paraformaldehyde (PFA) previous to in situ hybridization. The in situ hybridization protocol was adapted[37] using specific probes for the *iars* mRNAs. The MOs used were splice blocking and 5-bp-mismatch control MOs, designed and synthesized by Gene Tools (exon 18 MO: 5′-ATG TGTGGTTTGTTTTCTCACCGTA-3′, exon 18 5-bp-mismatch 5′-AT aTGTaGTTTaTTTTCTaACCaTA-3′; exon 32 MO: 5′-ACCGTCTGA CAGCAGAACACACAGA-3′, exon 32 5-bp mismatch: 5′-AaCGTC TaACAGaAGAACAaACAaA-3′). Single-cell stage embryos were injected with 0.5 ng of MO and maintained at 28°C until the desired developmental stage was attained.

Lateral views with anterior to the left at developmental stages indicated.

(A) In situ hybridization for *iars* mRNA at 13 hpf and sense mRNA control. *Iars* expression localizes predominantly to the somites and developing brain regions. The arrow indicates midbrain expression.

(B) 25 hpf. *Iars* in situ (left), arrows indicate tectum (blue), cerebellum (black), and somites (red). Sense control (right) shows no signal.

(C) 48 hpf. *Iars* is specifically expressed in the tectum region of the brain (blue), as well as in the pineal gland (green) and hindbrain (black).

(D) MO-injected zebrafish embryos at 26 hpf are shown. Knockdown of *iars* yields retarded development, brain deformity, as indicated by the arrow to the midbrain region, and severe shortening of the body axis, as highlighted by the double head arrows. Left, control embryo; middle, zebrafish injected with MO targeting exon 18; right, zebrafish injected with MO targeting exon 32.

validated by RT-PCR and injection of 5-bp-mismatch MOs (Figure 3 and data not shown). Upon *iars* downregulation, embryonic development is generally delayed, with embryos exhibiting altered brain configuration and severe shortening of the posterior body axis (Figure 3). The observed phenotype had a high consistency of about 85% for both MOs. Notably, the knockdown resulted in a concentration-dependent high level of lethality. Embryos injected with 0.5 ng and 1 ng MO targeting exon 32 showed 40% ($n = 35$) and 80% ($n = 95$) lethality rates, respectively, while 80% and 85% of embryos died upon injection of the same concentrations of MO targeting exon 18 ($n_{0.5ng} = 37$ and $n_{1ng} = 87$). Lethality rate was decreased to 41% ($n = 93$) by addition of human *IARS* mRNA, confirming the MO targeting exon 18 specificity and, at the same time, suggesting an evolutionarily conserved role for *iars* in embryonic development. As in yeast, zinc treatment did not result in a phenotypic rescue (data not shown). Overall the experiments performed in this animal model suggest an important role for Iars in embryogenesis. Downregulation of *iars* causes high lethality, with surviving embryos exhibiting a severe and consistent brain phenotype and a shortening of the body axis reminiscent of the human phenotype.

Mutations in *IARS* recently have been identified as underlying weak calf syndrome in Japanese black cattle.[8] The phenotype of the calf disorder strikingly resembles that of the three probands of this study. Body weight in six affected calves was between 30% and 70% of that of age-matched control calves. We tested whether oxidative phosphorylation (OXPHOS) activity is decreased in affected calves, as findings varied within our patient cohort. OXPHOS activities in muscle, liver, and fibroblasts of affected calves ($n = 6$) were normal compared with controls ($n = 3$; see Table S2). Thus, OXPHOS dysfunction is not directly linked to mutations in *IARS* in calves. We also determined blood zinc levels in 13 affected calves and 20 healthy calves. Zinc levels did not differ between the two groups (Table S3). Hence it is likely that reduced zinc levels and impaired OXPHOS activities are not directly related to *IARS* mutations.

Our genetic and experimental findings provide evidence that mutations affecting functionally conserved domains in *IARS* cause a multisystem phenotype in man including severe growth retardation with prenatal onset, intellectual disability, muscular hypotonia, and infantile hepatopathy.

All three individuals presented in this study share principal clinical features, but phenotypes vary. The neurological phenotype in individual #65269 (DEU) is severe, including absence of expressive speech, spasticity, pronounced white matter deficit, and severe microcephaly, whereas individual #85880 (JPN) has moderate intellectual

disability without motor dysfunction and with normal findings on brain MRI. It cannot be excluded that the intellectual disability of individual #85880 (JPN) is modified by another cause than *IARS* mutations, because her sister, who did not harbor the identified pathogenic *IARS* variants, is also affected by intellectual disability. However, in the families of individuals #65269 (DEU) and #83921 (AUT), family histories for intellectual disability are unremarkable.

Liver function was basically normal in individual #65269 (DEU), whereas infantile hepatopathy (leading to liver failure in one occasion) was present in the other two probands, with steatosis and portal-tract fibrosis. Liver biopsy of individual #83921 (AUT) additionally displayed cholestasis. Among 107 rare or private variants identified in the exome of this subject was a heterozygous c.1460G>A (p.Arg487His) change in *ABCB11* (MIM: 603201, GenBank: NM_003742), encoding bile salt export pump (BSEP). However, immunostaining of liver-biopsy material found normal BSEP marking. A homozygous mutation affecting the same codon, yielding p.Arg487Pro, has been identified in a subject with progressive familial intrahepatic cholestasis type 2 (MIM: 601847).[14] Heterozygous *ABCB11* mutations are implicated as predisposing to intrahepatic cholestasis of pregnancy[15] and to transient neonatal cholestasis.[16] The *ABCB11* variant identified in individual #83921 (AUT) may contribute to greater severity of liver disease, including cholestasis, in him than in the other individuals with compound heterozygous *IARS* mutations and no rare variants in *ABCB11*.

An essential role of IARS is underlined by the fact that none of the human subjects have two loss-of-function alleles (the same holds for affected calves, which are homozygous for a single substitution mutation) and by the mainly lethal, severe phenotype of MO knockdown zebrafish. The pathomechanism of IARS deficiency is not yet understood. Although reduced growth could be explained by altered global translational performance, the pathomechanism of organ-specific signs is likely to be more complex. Given the ubiquitous presence and vital importance of ARSs in all cells of archae, bacteria, and eukarya, it is remarkable that mutations in ARSs cause considerably distinct clinical pictures with tissue-specific phenotypes in humans.[1,4,17] Apart from aminoacylation and editing activity, the so-called canonical functions of ARSs, some ARSs exhibit non-canonical activities in vertebrates. These include translational control, transcription regulation, signal transduction, and modulation of cell migration, angiogenesis, inflammation, and tumorigenesis.[1,18] IARS also is part of a multi-synthetase complex (MSC), which is organized by nine cytoplasmic ARSs and the three aminoacyl-tRNA synthetase-interacting multifunctional proteins AIMP1, AIMP2, and AIMP3.[19,20] Tissue specificity has been speculatively linked to such non-canonical functions or to involvement in the MSC.[21] Interestingly, deficiencies of LARS and MARS also are known to cause hepatopathy,[6,7] and these enzymes also are part of the MSC. To propose a role of MSC dysfunction in hepatobiliary disease thus lies near at hand, perhaps through accumulation of mis-folded proteins, with endoplasmic-reticulum stress in consequence, due to incorrect editing of amino acids.[22] An important role for *iars* in zebrafish brain development is consonant with the abnormalities of brain function in the subjects of this study.

Regarding the MRI findings in cytosolic ARS, several open questions remain. The mild supratentorial white matter T2-hyperintensity in subject #65269 (DEU) is consistent either with a complex pattern of hypomyelination with a normal signal of subcortical, late myelinating white matter or with white matter changes secondary to neurodegeneration; his visually low choline resonances in the quantitiative MRS are also consistent with hypomyelination. The presumed hypomyelination may be compared with individuals with mutations in *DARS* (MIM: 603084),[23,24] whereas microcephaly is reminiscent of the phenotype seen in individuals with mutations in *QARS* (MIM: 603727).[25] A simplified gyral pattern is not apparent, however, in the individuals with mutations in *IARS*. The beneficial effect of zinc supplementation observed in human subjects could not be demonstrated in the yeast or zebrafish models. Therefore, IARS enzyme activity seems to be independent of zinc levels and the beneficial effect of zinc supplementation is likely compensating secondary zinc deficiency. However, zinc has been proposed to interact with the active site of IARS and to be required for normal cell growth.[13] A role for zinc, especially in editing substrate specificity, has been demonstrated for other ARSs, including alanyl-, seryl-, and threonyl-tRNA synthetase.[26–29] The cause of zinc deficiency as observed in all our three probands remains unresolved, but could be explained by chronic liver disease at least in individuals AUT and JPN, because chronic liver disease is known to be associated with zinc deficiency.[30,31]

In recent years, whole-exome sequencing studies have revealed various causes of infantile liver failure with partly specific clinical phenotypes, including mutations in *LARS*,[6] *NBAS* (MIM: 616483),[32,33] *SCYL1* (MIM: 616719),[34] and now *IARS*. Precise genetic and clinical phenotyping is crucial for both understanding these diseases and for suspecting and diagnosing them in the clinical setting. This study delineates mutations in *IARS* as underlying a multisystemic disease affecting mainly growth, brain, and liver. For reasons yet to be determined, this disease is associated with zinc deficiency and can be palliated by zinc supplementation.

## Supplemental Data

Supplemental Data include six figures and three tables and can be found with this article online at http://dx.doi.org/10.1016/j.ajhg.2016.05.027.

## Acknowledgments

We would like to thank the families for their collaboration. The authors thank Caterina Terrile, Masakazu Kohda, and Yoshihito

Kishita for excellent technical and bioinformatical assistance, Dr. Kai Hell for providing the TET-ILS1 yeast strain and pYX122 plasmid, and Dr. Takako Yoshioka for providing a liver-biopsy specimen from individual #85880 (JPN). The authors also thank Dr. Shigeru Toyoda and Dr. Takahiro Tahara for referral of subject materials and Dr. M. Meissl, who attends individual #83921 (AUT). This work was supported by the German Bundesministerium für Bildung und Forschung (BMBF) through the E-Rare project GENOMIT (01GM1207) and the German Network for Mitochondrial Disorders (mitoNET; 01GM1113C). T.B.H. was supported by the BMBF through the Juniorverbund in der Systemmedizin "mitOmics" (FKZ 01ZX1405C) and H.P. by EU FP7 Mitochondrial European Educational Training Project (317433) and EU Horizon2020 Collaborative Research Project SOUND (633974). This work was further supported by a grant of the Practical Research Project for Rare/Intractable Diseases from Japan Agency for Medical Research and Development (AMED) to K.M., the Innovative Cell Biology by Innovative Technology (Cell Innovation Program) from the Ministry of Education, Culture, Sports, Science and Technology (MEXT), Japan to Y.O.; the Support Project and a grant of Strategic Research Center in Private Universities from MEXT, Japan to Saitama Medical University Research Center for Genomic Medicine; and the Grant-in-Aid (27008B) for Japan Science and technology research promotion program for agriculture, forestry, fisheries, and food industry to D.W. for research on affected Japanese calves.

Received: January 14, 2016
Accepted: May 25, 2016
Published: July 14, 2016

## Web Resources

ExAC Browser, http://exac.broadinstitute.org/
GenBank, http://www.ncbi.nlm.nih.gov/genbank/
Japan Agency for Medical Research and Development (AMED), http://www.amed.go.jp/
Ministry of Education, Culture, Sports, Science and Technology, Cell Innovation Program, http://cell-innovation.nig.ac.jp/mext-life/english/index.html
Ministry of Education, Culture, Sports, Science and Technology, Support Project and Grant, http://www.mext.go.jp/a_menu/koutou/shinkou/07021403/002/002/1218299.htm
MutationTaster, http://www.mutationtaster.org/
OMIM, http://www.omim.org/

## References

1. Yao, P., and Fox, P.L. (2013). Aminoacyl-tRNA synthetases in medicine and disease. EMBO Mol. Med. *5*, 332–343.
2. Antonellis, A., Ellsworth, R.E., Sambuughin, N., Puls, I., Abel, A., Lee-Lin, S.Q., Jordanova, A., Kremensky, I., Christodoulou, K., Middleton, L.T., et al. (2003). Glycyl tRNA synthetase mutations in Charcot-Marie-Tooth disease type 2D and distal spinal muscular atrophy type V. Am. J. Hum. Genet. *72*, 1293–1299.
3. Diodato, D., Ghezzi, D., and Tiranti, V. (2014). The mitochondrial aminoacyl tRNA synthetases: genes and syndromes. Int. J. Cell Biol. *2014*, 787956.
4. Konovalova, S., and Tyynismaa, H. (2013). Mitochondrial aminoacyl-tRNA synthetases in human disease. Mol. Genet. Metab. *108*, 206–211.
5. Abbott, J.A., Francklyn, C.S., and Robey-Bond, S.M. (2014). Transfer RNA and human disease. Front. Genet. *5*, 158.
6. Casey, J.P., McGettigan, P., Lynam-Lennon, N., McDermott, M., Regan, R., Conroy, J., Bourke, B., O'Sullivan, J., Crushell, E., Lynch, S., and Ennis, S. (2012). Identification of a mutation in LARS as a novel cause of infantile hepatopathy. Mol. Genet. Metab. *106*, 351–358.
7. Hadchouel, A., Wieland, T., Griese, M., Baruffini, E., Lorenz-Depiereux, B., Enaud, L., Graf, E., Dubus, J.C., Halioui-Louhaichi, S., Coulomb, A., et al. (2015). Biallelic mutations of methionyl-tRNA synthetase cause a specific type of pulmonary alveolar proteinosis prevalent on Réunion island. Am. J. Hum. Genet. *96*, 826–831.
8. Hirano, T., Kobayashi, N., Matsuhashi, T., Watanabe, D., Watanabe, T., Takasuga, A., Sugimoto, M., and Sugimoto, Y. (2013). Mapping and exome sequencing identifies a mutation in the IARS gene as the cause of hereditary perinatal weak calf syndrome. PLoS ONE *8*, e64036.
9. Ogata, Y., Nakao, T., Takahashi, K., Abe, H., Misawa, T., Urushiyama, Y., and Sakai, J. (1999). Intrauterine growth retardation as a cause of perinatal mortality in Japanese black beef calves. Zentralbl. Veterinarmed. A *46*, 327–334.
10. Kornblum, C., Nicholls, T.J., Haack, T.B., Schöler, S., Peeva, V., Danhauser, K., Hallmann, K., Zsurka, G., Rorbach, J., Iuso, A., et al. (2013). Loss-of-function mutations in MGME1 impair mtDNA replication and cause multisystemic mitochondrial disease. Nat. Genet. *45*, 214–219.
11. Elstner, M., Andreoli, C., Klopstock, T., Meitinger, T., and Prokisch, H. (2009). The mitochondrial proteome database: MitoP2. Methods Enzymol. *457*, 3–20.
12. Mnaimneh, S., Davierwala, A.P., Haynes, J., Moffat, J., Peng, W.-T., Zhang, W., Yang, X., Pootoolal, J., Chua, G., Lopez, A., et al. (2004). Exploration of essential gene functions via titratable promoter alleles. Cell *118*, 31–44.
13. Landro, J.A., and Schimmel, P. (1994). Zinc-dependent cell growth conferred by mutant tRNA synthetase. J. Biol. Chem. *269*, 20217–20220.
14. Strautnieks, S.S., Byrne, J.A., Pawlikowska, L., Cebecauerová, D., Rayner, A., Dutton, L., Meier, Y., Antoniou, A., Stieger, B., Arnell, H., et al. (2008). Severe bile salt export pump deficiency: 82 different ABCB11 mutations in 109 families. Gastroenterology *134*, 1203–1214.
15. Dixon, P.H., van Mil, S.W., Chambers, J., Strautnieks, S., Thompson, R.J., Lammert, F., Kubitz, R., Keitel, V., Glantz, A., Mattsson, L.A., et al. (2009). Contribution of variant alleles of ABCB11 to susceptibility to intrahepatic cholestasis of pregnancy. Gut *58*, 537–544.
16. Hermeziu, B., Sanlaville, D., Girard, M., Léonard, C., Lyonnet, S., and Jacquemin, E. (2006). Heterozygous bile salt export pump deficiency: a possible genetic predisposition to transient neonatal cholestasis. J. Pediatr. Gastroenterol. Nutr. *42*, 114–116.
17. Antonellis, A., and Green, E.D. (2008). The role of aminoacyl-tRNA synthetases in genetic diseases. Annu. Rev. Genomics Hum. Genet. *9*, 87–107.
18. Guo, M., Schimmel, P., and Yang, X.L. (2010). Functional expansion of human tRNA synthetases achieved by structural inventions. FEBS Lett. *584*, 434–442.
19. Park, S.G., Ewalt, K.L., and Kim, S. (2005). Functional expansion of aminoacyl-tRNA synthetases and their interacting factors: new perspectives on housekeepers. Trends Biochem. Sci. *30*, 569–574.

20. Park, S.G., Choi, E.C., and Kim, S. (2010). Aminoacyl-tRNA synthetase-interacting multifunctional proteins (AIMPs): a triad for cellular homeostasis. IUBMB Life *62*, 296–302.
21. Park, S.G., Schimmel, P., and Kim, S. (2008). Aminoacyl tRNA synthetases and their connections to disease. Proc. Natl. Acad. Sci. USA *105*, 11043–11049.
22. Casey, J.P., Slattery, S., Cotter, M., Monavari, A.A., Knerr, I., Hughes, J., Treacy, E.P., Devaney, D., McDermott, M., Laffan, E., et al. (2015). Clinical and genetic characterisation of infantile liver failure syndrome type 1, due to recessive mutations in LARS. J. Inherit. Metab. Dis. *38*, 1085–1092.
23. Taft, R.J., Vanderver, A., Leventer, R.J., Damiani, S.A., Simons, C., Grimmond, S.M., Miller, D., Schmidt, J., Lockhart, P.J., Pope, K., et al. (2013). Mutations in DARS cause hypomyelination with brain stem and spinal cord involvement and leg spasticity. Am. J. Hum. Genet. *92*, 774–780.
24. Wolf, N.I., Toro, C., Kister, I., Latif, K.A., Leventer, R., Pizzino, A., Simons, C., Abbink, T.E., Taft, R.J., van der Knaap, M.S., and Vanderver, A. (2015). DARS-associated leukoencephalopathy can mimic a steroid-responsive neuroinflammatory disorder. Neurology *84*, 226–230.
25. Zhang, X., Ling, J., Barcia, G., Jing, L., Wu, J., Barry, B.J., Mochida, G.H., Hill, R.S., Weimer, J.M., Stein, Q., et al. (2014). Mutations in QARS, encoding glutaminyl-tRNA synthetase, cause progressive microcephaly, cerebral-cerebellar atrophy, and intractable seizures. Am. J. Hum. Genet. *94*, 547–558.
26. Sankaranarayanan, R., Dock-Bregeon, A.C., Romby, P., Caillet, J., Springer, M., Rees, B., Ehresmann, C., Ehresmann, B., and Moras, D. (1999). The structure of threonyl-tRNA synthetase-tRNA(Thr) complex enlightens its repressor activity and reveals an essential zinc ion in the active site. Cell *97*, 371–381.
27. Sankaranarayanan, R., Dock-Bregeon, A.C., Rees, B., Bovee, M., Caillet, J., Romby, P., Francklyn, C.S., and Moras, D. (2000). Zinc ion mediated amino acid discrimination by threonyl-tRNA synthetase. Nat. Struct. Biol. *7*, 461–465.
28. Bilokapic, S., Maier, T., Ahel, D., Gruic-Sovulj, I., Söll, D., Weygand-Durasevic, I., and Ban, N. (2006). Structure of the unusual seryl-tRNA synthetase reveals a distinct zinc-dependent mode of substrate recognition. EMBO J. *25*, 2498–2509.
29. Pasman, Z., Robey-Bond, S., Mirando, A.C., Smith, G.J., Lague, A., and Francklyn, C.S. (2011). Substrate specificity and catalysis by the editing active site of Alanyl-tRNA synthetase from *Escherichia coli*. Biochemistry *50*, 1474–1482.
30. Narkewicz, M.R., Krebs, N., Karrer, F., Orban-Eller, K., and Sokol, R.J. (1999). Correction of hypozincemia following liver transplantation in children is associated with reduced urinary zinc loss. Hepatology *29*, 830–833.
31. Umusig-Quitain, P., and Gregorio, G.V. (2010). High incidence of zinc deficiency among Filipino children with compensated and decompensated liver disease. J. Gastroenterol. Hepatol. *25*, 387–390.
32. Haack, T.B., Staufner, C., Köpke, M.G., Straub, B.K., Kölker, S., Thiel, C., Freisinger, P., Baric, I., McKiernan, P.J., Dikow, N., et al. (2015). Biallelic mutations in NBAS cause recurrent acute liver failure with onset in infancy. Am. J. Hum. Genet. *97*, 163–169.
33. Staufner, C., Haack, T.B., Köpke, M.G., Straub, B.K., Kölker, S., Thiel, C., Freisinger, P., Baric, I., McKiernan, P.J., Dikow, N., et al. (2016). Recurrent acute liver failure due to NBAS deficiency: phenotypic spectrum, disease mechanisms, and therapeutic concepts. J. Inherit. Metab. Dis. *39*, 3–16.
34. Schmidt, W.M., Rutledge, S.L., Schüle, R., Mayerhofer, B., Züchner, S., Boltshauser, E., and Bittner, R.E. (2015). Disruptive SCYL1 mutations underlie a syndrome characterized by recurrent episodes of liver failure, peripheral neuropathy, cerebellar atrophy, and ataxia. Am. J. Hum. Genet. *97*, 855–861.
35. Westerfield, M. (2000). The Zebrafish Book. A Guide for the Laboratory Use of Zebrafish (*Danio rerio*), Fourth Edition (Eugene: University of Oregon Press).
36. Kimmel, C.B., Ballard, W.W., Kimmel, S.R., Ullmann, B., and Schilling, T.F. (1995). Stages of embryonic development of the zebrafish. Dev. Dyn. *203*, 253–310.
37. Thisse, C., and Thisse, B. (2008). High-resolution in situ hybridization to whole-mount zebrafish embryos. Nat. Protoc. *3*, 59–69.

**The American Journal of Human Genetics, Volume *99***

## Supplemental Data

# Biallelic *IARS* Mutations Cause Growth Retardation with Prenatal Onset, Intellectual Disability, Muscular Hypotonia, and Infantile Hepatopathy

**Robert Kopajtich, Kei Murayama, Andreas R. Janecke, Tobias B. Haack, Maximilian Breuer, A.S. Knisely, Inga Harting, Toya Ohashi, Yasushi Okazaki, Daisaku Watanabe, Yoshimi Tokuzawa, Urania Kotzaeridou, Stefan Kölker, Sven Sauer, Matthias Carl, Simon Straub, Andreas Entenmann, Elke Gizewski, René G. Feichtinger, Johannes A. Mayr, Karoline Lackner, Tim M. Strom, Thomas Meitinger, Thomas Müller, Akira Ohtake, Georg F. Hoffmann, Holger Prokisch, and Christian Staufner**

**Figure S1. Growth curves, individual #65269 (DEU)**

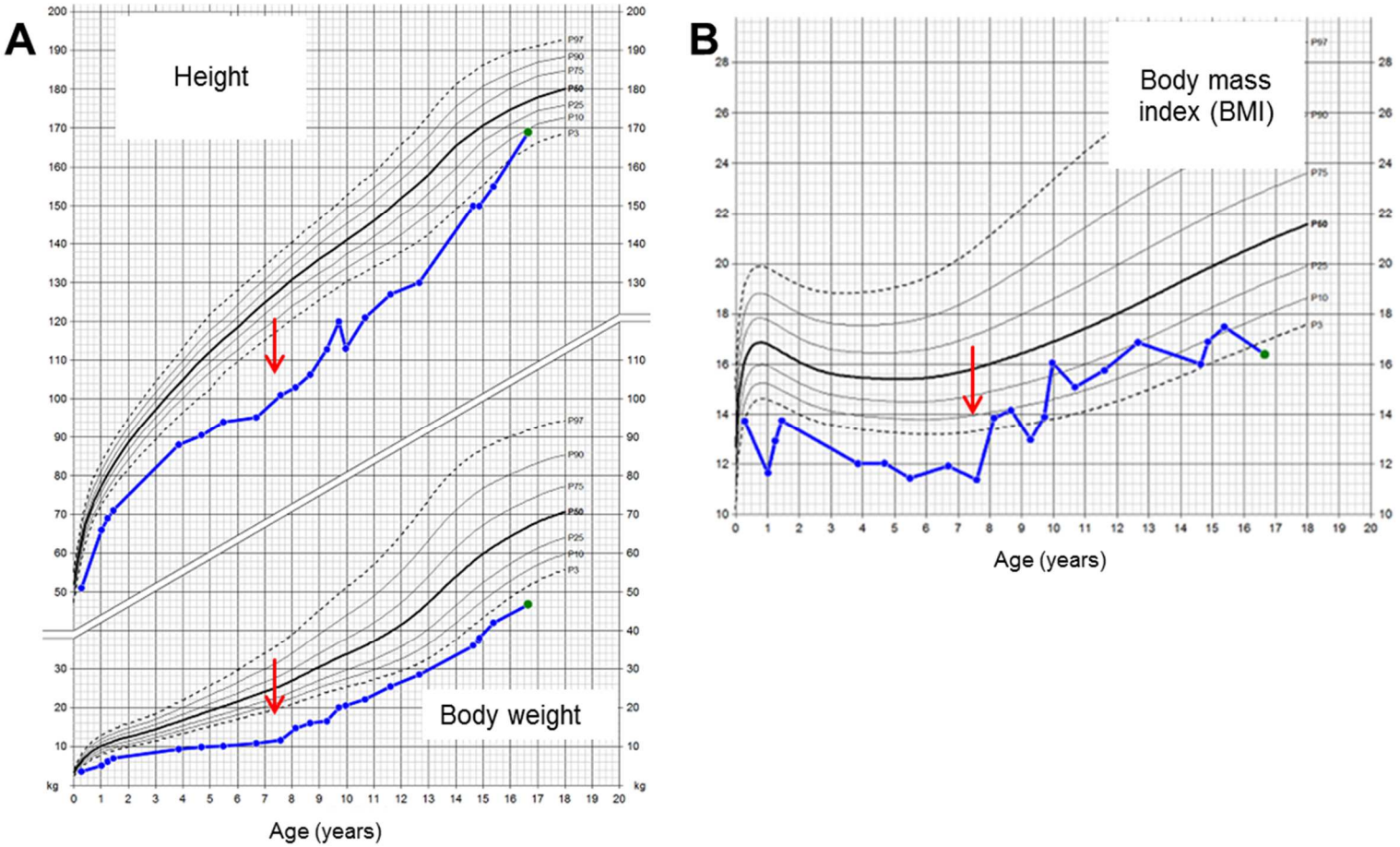


Curves of height (top) and body weight (bottom) (A) and body mass index (BMI) (B) of subject #65269 (DEU). Severe growth retardation and failure to thrive were at their worst at 7 years of age, when zinc deficiency was detected and supplementary treatment with 10mg zinc/day was initiated (0.9 mg/kg body weight/day; red arrow). After zinc supplementation began, the patient gained 3 kg in the first six months and BMI rose from 11.4 kg/m² (-4.2 SDS) to 13.9 kg/m² (-1.5 SDS).

**Figure S2. Brain magnetic-resonance images, individual #65269 (DEU), age 17 years**

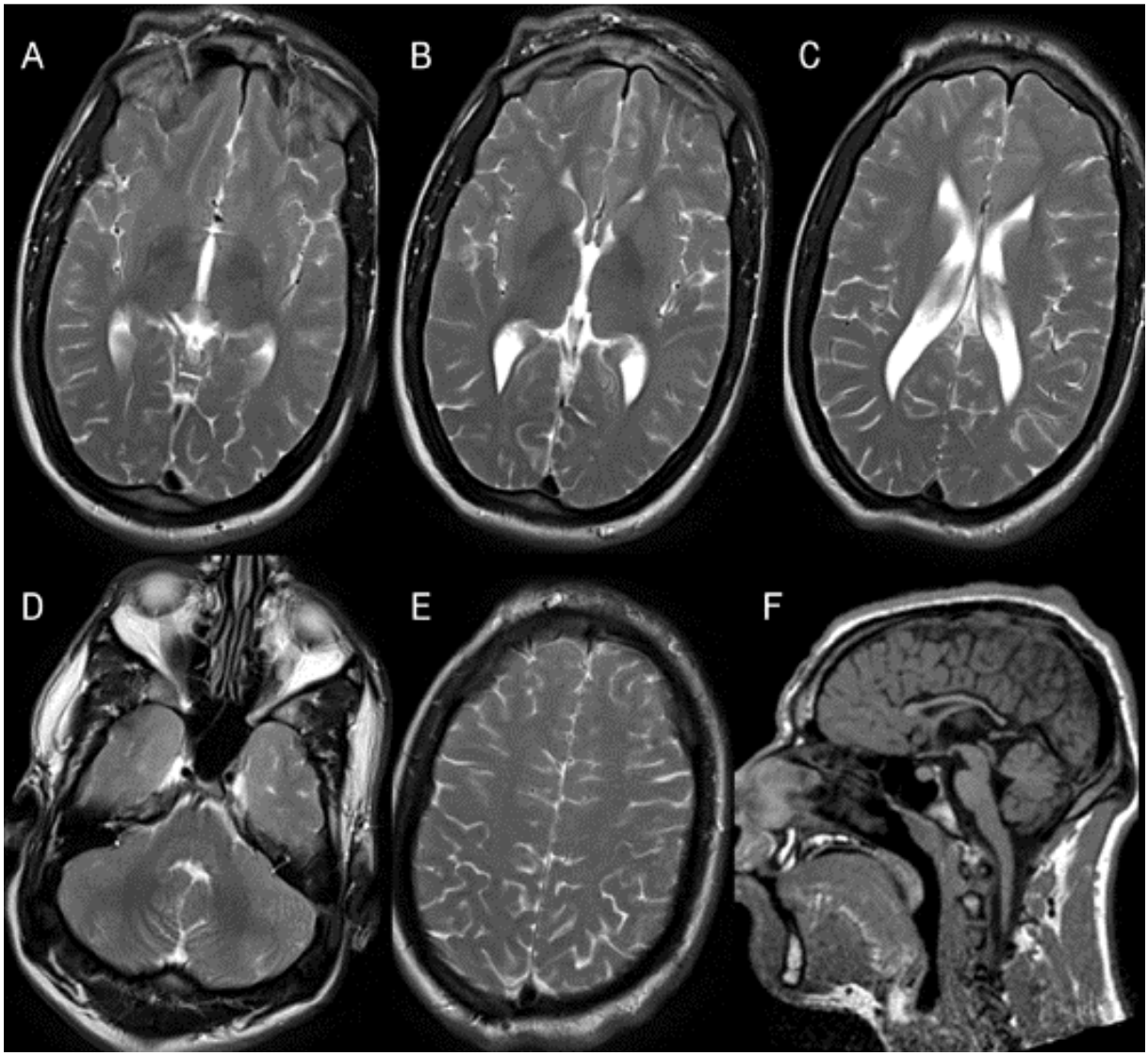


A-E: T2-weighted axial images depicting hazy T2-hyperintensity of supratentorial white matter with sparing of the subcortical temporal (D) and frontal (A, B) white matter, which has the normal hypointense signal of myelinated white matter. The supratentorial corticospinal tract is involved from the Rolandic area (E) through the corona radiata and posterior limb of the internal capsule (B, C). A thin periventricular rim is spared (B, C). Microcephaly is present, with a neurocranium disproportionately small compared with the viscerocranium on the midsagittal T1-weighted image (F). There is a deficit of supratentorial white matter with widened lateral ventricles (C) and a thin corpus callosum (F).

Brain images of #85880 (JPN) and #83921 (AUT) have been evaluated together with those of individual #65269 (DEU). They were normal at the respective ages of 16 and 2 years.

**Figure S3. Liver biopsy, individual #85880 (JPN), age 2 1/12 years**

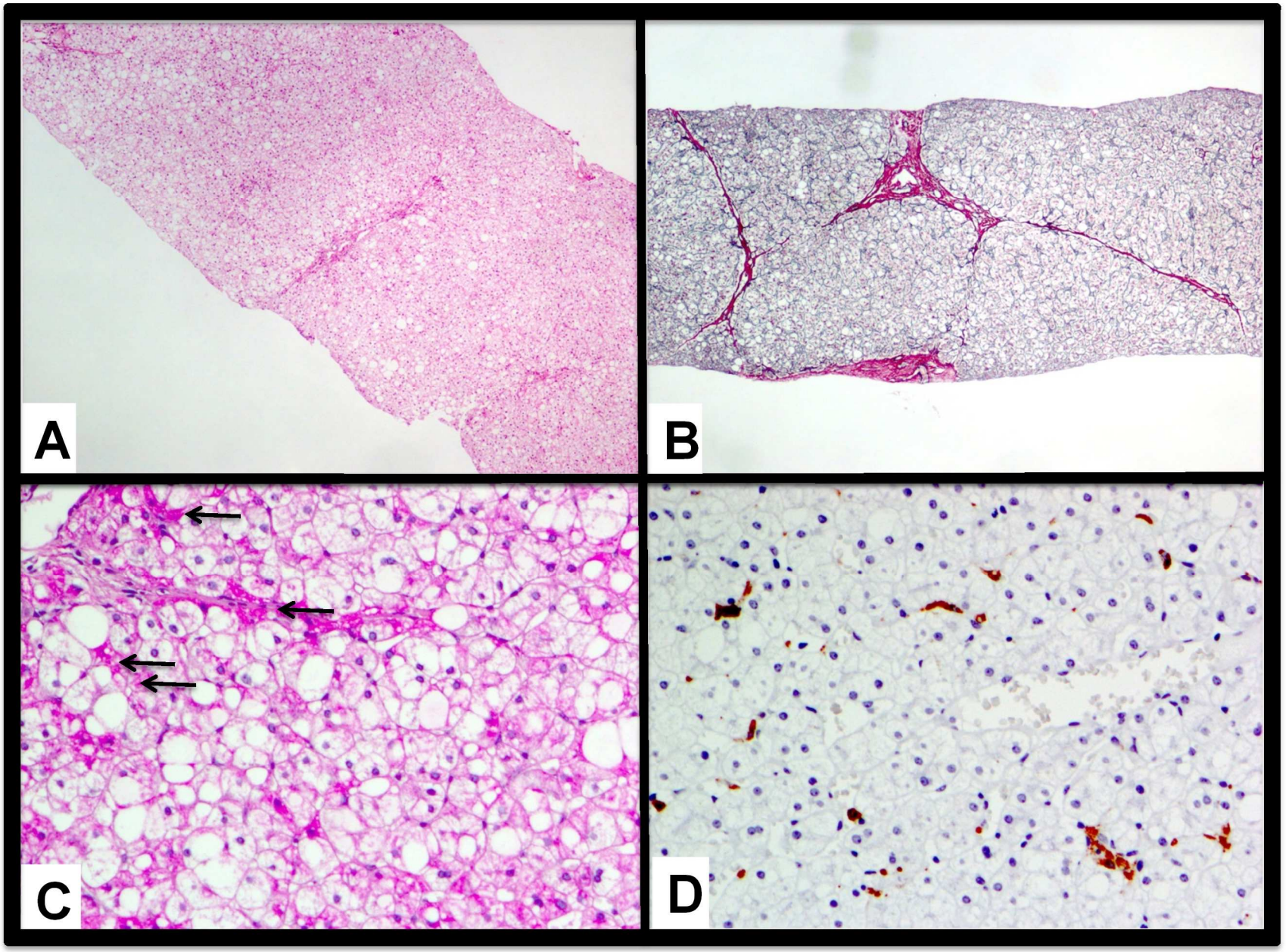

Steatosis and portal-tract fibrosis with evidence of accelerated hepatocyte turn-over in absence of other usual histopathologic features of hepatitis or steatohepatitis. Lymphoplasmacytic or granulocytic inflammation is not observed; ballooning and Mallory-Denk bodies are not seen. Cholestasis, copper accumulation, and siderosis are not found. (A) Hepatocyte pallor and delicate bridging fibrosis; inflammation is not a feature. Hematoxylin / eosin, original magnification 40x. (B) Fibrosis with bridging. Reticulin, original magnification 40x. (C) Small- and large-droplet steatosis displaces purplish glycogen within cytoplasm of hepatocytes. Purplish ceroid pigment is seen in some Kupffer cells and macrophages (arrows). Periodic acid - Schiff reaction / hematoxylin, original magnification 200x. (D) Clusters of dark brown Kupffer cells correspond to ceroid-laden cells in C, above; such accumulations mark sites of cell death and phagocytic response. Anti-macrosialin / -CD68 antibody – diaminobenzidine / hematoxylin, original magnification 200x.

**Figure S4. Liver biopsy, individual #83921 (AUT), age 1 2/12 years**

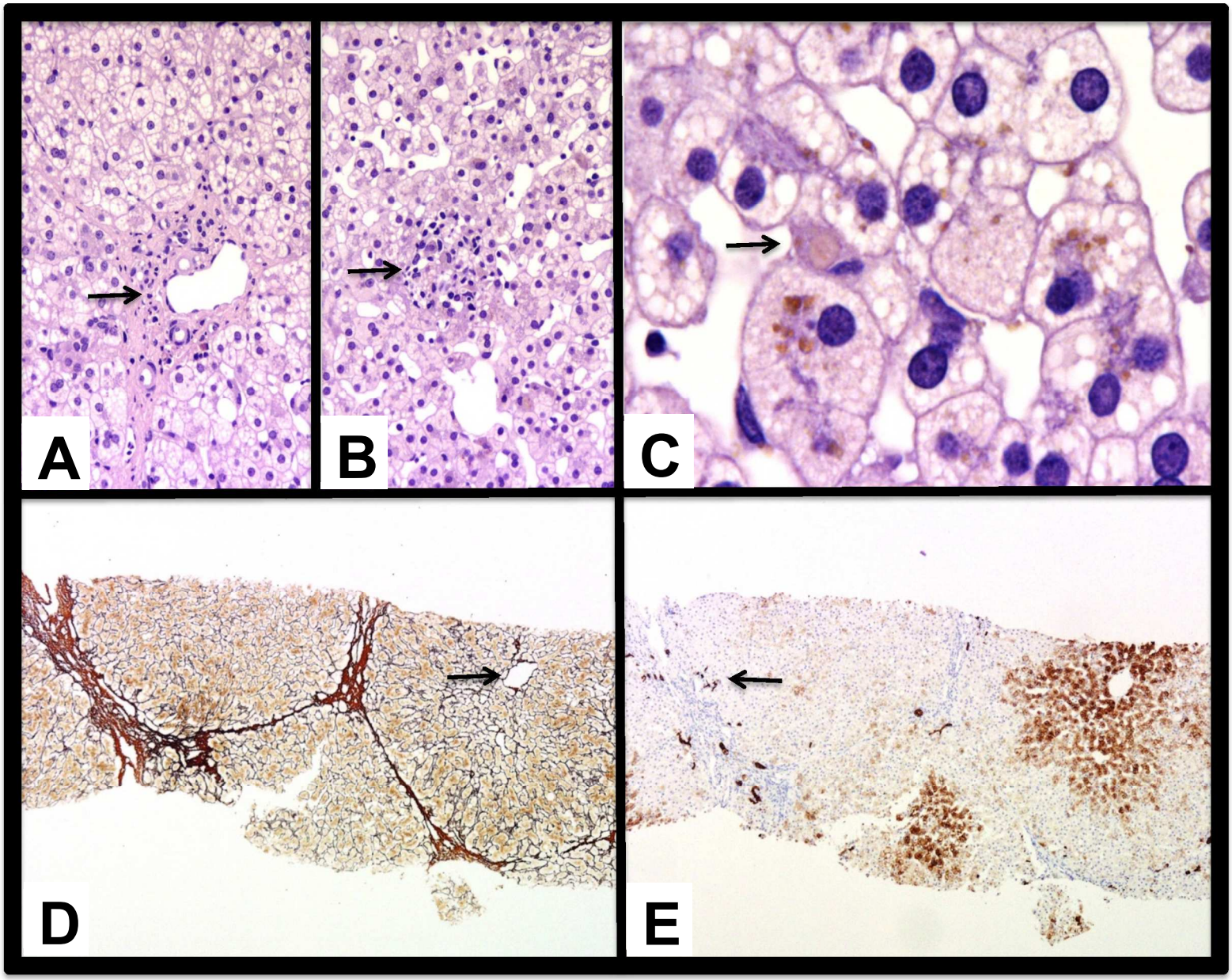

Cholestasis, steatosis with steatohepatitis, portal-tract fibrosis with bridging in biliary rather than post-necrotic pattern, and evidence of accelerated hepatocyte turn-over. Lymphoplasmacytic or granulocytic inflammation is not observed; ballooning and Mallory-Denk bodies are not seen. Copper accumulation and siderosis are not found. (A) and (B) Hepatocyte pallor and vacuolation. A portal tract (arrow, A) is free of inflammation, but a focus of mononuclear (phagocytic) response to necrosis (arrow, B) lies near a draining venule. Hematoxylin / eosin (H&E), original magnification 200x. (C) Hepatocellular steatosis; a Kupffer cell containing ceroid pigment is noted (arrow). Hepatocyte cytoplasm contains flecks of bile pigment. H&E, original magnification 1,000x. (D) Moderate and mild portal-tract fibrosis with extensive portal-portal bridging fibrosis. A draining venule (arrow) is unremarkable. Reticulin, original magnification 40x. (E) Dark brown neocholangioles (“ductular reaction”) highlighted as expressing cytokeratin (CK) 7 are seen at margins of damaged portal tracts (arrow). Heterotopic expression of CK7 by hepatocytes, a feature of chronic cholestasis, is widespread. Anti-CK7 antibody – diaminobenzidine / hematoxylin, original magnification 40x.

**Figure S5. Immunoblotting analysis of liver and muscle (individual #83921, AUT) and fibroblasts (individual #83921, AUT; individual #65269, DEU; individual #85880, JPN)**

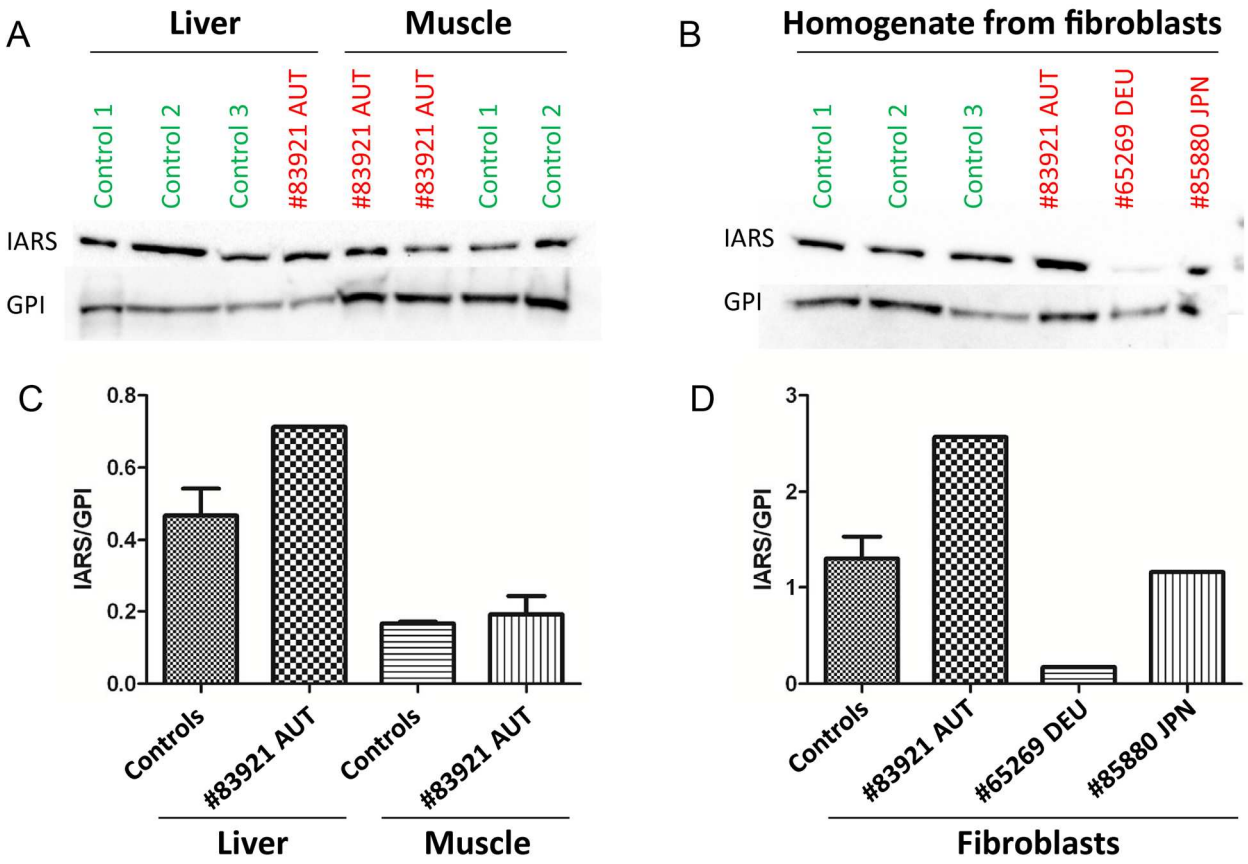


Western blot analysis with 600 g supernatants from (A) liver and muscle and (B) homogenates from fibroblasts was performed with antibodies against IARS (Anti-IARS, Rabbit; Biomol, Cat.-No. A304-748A-T) and GPI (glucose-6-phosphate isomerase) as loading control. Quantitative analysis (C, D) revealed a normal relative amount of IARS/ GPI in all samples of individuals #83921 (AUT) and #85880 (JPN), while a decreased amount of IARS protein was found in fibroblasts of #65269 (DEU).

**Figure S6. Immunostaining of liver-biopsy materials from individual #83921 (AUT) and individual #85880 (JPN) for IARS**

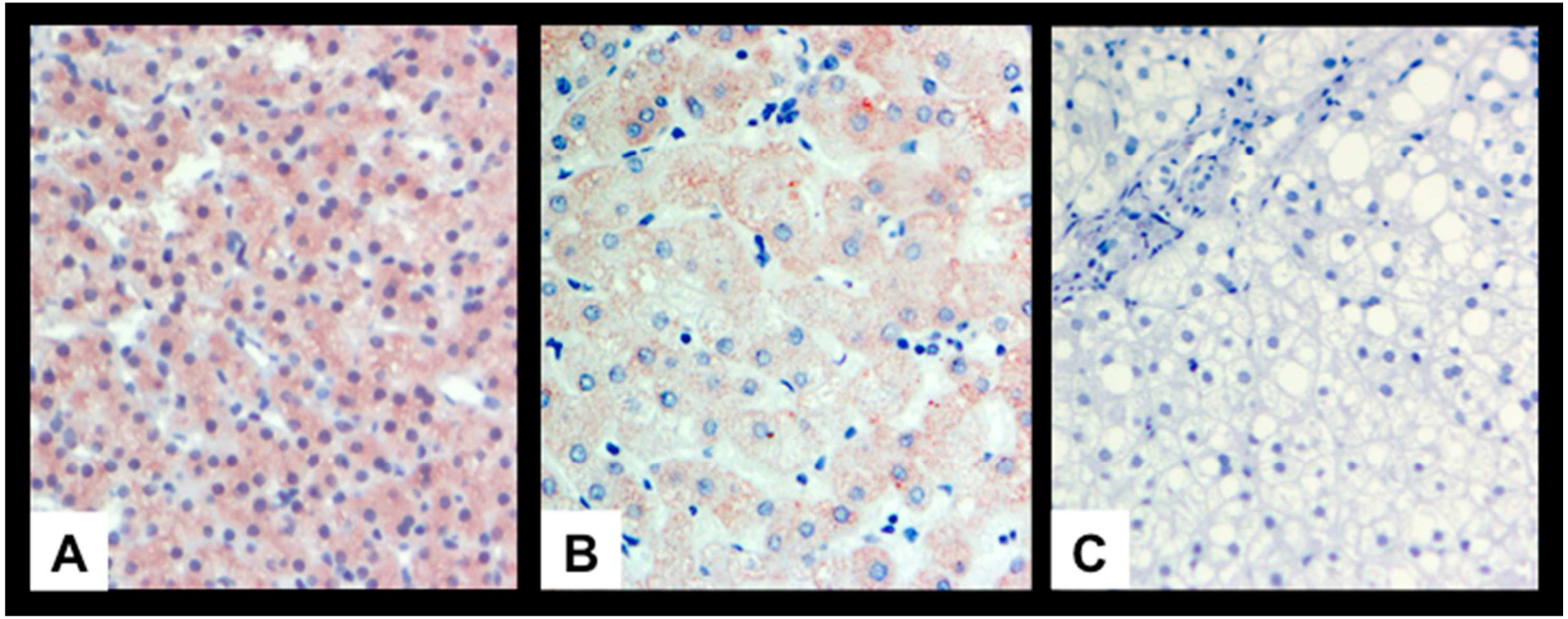


(A) AUT. Hepatocyte cytoplasm marks diffusely. (B) A liver control. Marking is apparent in both A and B; variation in intensity is apparent, and is likely multifactorial. (C) JPN. No marking for IARS is seen. Anti-IARS / hematoxylin, original magnification 200x, all images.

## SUPPLEMENTAL TABLES

**Table S1. Anthropometrical data**

| | | | at birth | | | at one year | | | at six years | | | at current age | | | |
|---|---|---|---|---|---|---|---|---|---|---|---|---|---|---|---|
| **ID** | sex | gestational age at birth (weeks) | length (cm/SDS) | weight (g/SDS) | head circumference (cm/SDS) | height (cm/SDS) | weight (kg/SDS) | head circumference (cm/SDS) | height (cm/SDS) | weight (kg/SDS) | head circumference (cm/SDS) | age | height (cm/SDS) | weight (kg/SDS) | head circumference (cm/SDS) |
| #65269 (DEU) | m | 38 | 45/-2.7 | 2020 / -3.0 | 29 / -4.2 | 66 / -4.4 | 5.1 / -4.7 | 38 / -8.1 | 95.2 / -5.9 | 10.8 / -8.0 | 42 / -7.4 | 18 y | 169 / -1.6 | 50.0 / -2.8 | 48.5 / -5.1 |
| #85880 (JPN) | f | 38 | 42/ -2.7 | 1564 / -4.1 | 29 / -3.5 | 58 / -6.2 | 4.5 / -4.2 | 38 / -4.1 | 100.0 / -2.8 | 16.0 / -1.2 | n.a. | 19 y | 155 / -0.6 | 46.2 / -0.9 | “normal” |
| #83921 (AUT) | m | 38+4 | 48/-1.6 | 2700 / -1.6 | 30 / -3.8 | n.a. | n.a. | n.a. | n.a. | n.a. | n.a. | 3y | 82 / -5.0 | 11.5 / -2.0 | 47 / -3.3 |

f, female; m, male; SDS, standard deviation score; n.a., not available

**Table S2. OXPHOS activities**

| ID | RCC | % of lowest control / absolute values / reference range |
|---|---|---|
| #65269 (DEU) | **Muscle** | |
| | I | **77%** / 65 mU/U CS / 84-273 |
| | II | n.a. |
| | II+III | normal / 9.7 mU/mg protein / 4.2-29 |
| | IV | **52%** / 270 mU/U CS / 520-2080 |
| | PDH | **64%** / 18.7 mU/U CS / 29-89 |
| | **Liver** | not done |
| | **Fibroblasts** | all normal |
| #85880 (JPN) | **Muscle** | not done |
| | **Liver** | not done |
| | **Fibroblasts** | |
| | I | **73%** / 196 mU/U CS / 267-792 |
| | II | normal / 423 mU/U CS / 299-1162 |
| | II+III | normal / 381 mU/U CS / 346-1281 |
| | III | normal / 144 mU/U CS / 22-281 |
| | IV | normal / 14.0 mU/U CS / 14-64 |
| | PDH | n.a. |
| #83921 (AUT) | **Muscle** | all normal, including PDH |
| | **Liver** | |
| | I | **46%** / 70 mU/U CS / 150–370 |
| | II | normal / 970 mU/U CS / 780-1172 |
| | I+III | normal / 540 mU/U CS / 260-610 |
| | III | normal / 6950 mU/U CS / 1670-5170 |
| | IV | normal / 3210 mU/U CS / 880-1580 |
| | V | normal / 1810 mU/U CS / 350-1340 |
| | PDH | n.a. |
| | **Fibroblasts** | not done |
| weak calf syndrome (n=6) | **Muscle** | |
| | I | normal / 190 (153-274) mU/U CS / 77-512 |
| | II | normal / 146 (66-233) mU/U CS / 66-450 |
| | II+III | normal / 239 (103-233) mU/U CS / 88-584 |
| | III | normal / 50 (24-79) mU/U CS / 15-100 |
| | IV | normal / 41 (32-51) mU/U CS / 11-72 |
| | PDH | n.a. |
| | **Liver** | |
| | I | normal / 1134 (665-1598) mU/U CS / 299-1494 |
| | II | normal / 2232 (1634-2678) mU/U CS / 465-2324 |
| | III | normal / 326 (202-555) mU/U CS / 133-332 |
| | IV | normal / 258 (166-359) mU/U CS / 26-130 |
| | PDH | n.a. |
| | **Fibroblasts** | |
| | I | normal / 342 (240-449) mU/U CS / 109-544 |
| | II | normal / 477 (141-954) mU/U CS / 127-638 |
| | II+III | normal / 532 (450-84) mU/U CS / 339-1696 |
| | III | normal* / 43 (13-75) mU/U CS / 19-94 |
| | IV | normal / 57 (49-69) mU/U CS / 19-94 |
| | PDH | n.a. |
| | | * In one IARS calf complex III activity was low (13 mU/U CS) |

**Table S3. Zinc levels, weak calf syndrome and controls**

| Age | Plasma zinc in µg/dL - affected calves | n | Plasma zinc in µg/dL - healthy calves | n |
|---|---|---|---|---|
| 0-3 months | 139.3 (SD 60.7) | 4 | 116.6 (SD 21.4) | 10 |
| 4-9 months | 93.6 (SD 19.5) | 7 | 112.2 (SD 20.7) | 10 |
| >12 months | 109.4 (SD 10.6) | 5 | | |
| Age unknown | 107.0 (SD 24.0) | 2 | | |